Monostatic Backscatter System with Multi-Tag to Reader Communication

Jing Guo, Salman Durrani, *Senior Member, IEEE* and Xiangyun Zhou, *Senior Member, IEEE*

***Abstract*— In this work, we consider a monostatic backscatter communication system employing successive interference cancellation where a reader simultaneously serves multiple backscatter tags or nodes (BNs). To minimise collisions, each BN randomly chooses a sub-frame to backscatter the continuous wave signal transmitted by the reader only if its received power is above a backscatter threshold. The reader then employs successive interference cancellation technique to resolve the resulting smaller number of collisions. Using stochastic geometry, we derive an approximate yet accurate expression for the average number of successfully decoded BNs. Our derived expression allows the system performance to be predicted numerically and also allows us to determine the backscatter threshold to maximize the system performance.**

***Index Terms*—Backscatter communication, successive interference cancellation, stochastic geometry, Poisson point process.**

I. Introduction

Next generation Backscatter communication (BackCom) systems, which allow a tag or node to transmit data by reflecting and modulating an incident RF wave, are expected to play a key role in the future Internet-of-things [1], [2]. In this regard, multiple-access monostatic BackCom systems, where a single reader decodes information from multiple backscatter tags or nodes (BNs), have attracted a lot of recent attention [3]–[6]. The key challenge in such systems is how to deal with the collisions when two or more nodes backscatter at the same time. The performance of a backscatter sensor network where frequency modulation and directive antennas were employed to reduce the collisions was analyzed in [3]. A collision avoidance approach based on compressive sensing was developed in [4]. An energy beamforming scheme was proposed in [5] to avoid collisions, with the BNs accessing the reader in a time division multiple access fashion. A non-orthogonal multiple access pairing scheme for near and far nodes was proposed in [6], to enable the reader to distinguish transmissions from two paired BNs with suitably designed reflection coefficients. A limitation of all of the above works is that they assume the number of BNs is fixed.

In some use cases the number of BNs can be random, e.g., in sensor networks when a large number of BNs are deployed. The probability of being decoded for a typical BN with different collision resolution methods, i.e., directional antennas, successive interference cancellation (SIC) and ultra-narrow band transmissions, was investigated in [7] by modelling the BNs as a Poisson Point Process (PPP). Similar to [7], as a relatively amenable technique [8], [9], the SIC is also considered in this work to reduce the collision caused by multiple BNs. However, for the SIC technique in [7], the authors did not investigate any mechanism to improve the system performance by utilizing the property of BackCom system. This important shortcoming is addressed in this work.

Contributions: The major contributions of this work are: (i) To minimise the number of collisions in a multiple-access monostatic BackCom system, we introduce the concept of a backscatter threshold, i.e., each BN randomly chooses a sub-frame to backscatter its signal only if the received power is above the backscatter threshold. By first ensuring that only a few nodes collide at any time, any collisions are then efficiently resolved by the reader using SIC. This idea makes use of the BackCom system's characteristic; (ii) We leverage stochastic geometry and propose an approximate yet accurate analytical framework to evaluate the overall network performance in terms of the average number of successfully decoded BNs. Compared to existing literature, the proposed framework provides more accurate results in the relatively low signal-to-interference-plus-noise ratio (SINR) threshold region and the scenario with smaller number of accessing BNs; (iii) Our results show that there is an optimal backscatter threshold which maximizes the system performance. Additionally, the number of sub-frames needs to be selected carefully to minimise the underutilization of sub-frames while operating at close to the best system performance.

II. System Model

Consider a monostatic BackCom system with a single reader and multiple BNs. Let the reader be located at the origin o and the BNs be denoted by a PPP $\Phi = \{x_i\}$ in $\mathbb{R}^2$, where x represents the location of a BN. In general, the BNs are more likely to be clustered around the reader. Hence, we adopt a clustered network model from [8], i.e., the density function of BNs is given by $\lambda(x) = \bar{\lambda}||x||^b$, where $||x||$ denotes the distance between a BN and the reader and $b \in (-2, 0)$. The reader is transmitting the continuous wave (CW) signal all the time and its transmit power is denoted by P_T. The self-interference from the reader is assumed to be removed. All the wireless links experience the path-loss plus the identically distributed (i.i.d.) Nakagami-m block fading. Let α and h

Copyright (c) 2015 IEEE. Personal use of this material is permitted. However, permission to use this material for any other purposes must be obtained from the IEEE by sending a request to pubs-permissions@ieee.org.

J. Guo is with the School of Information and Electronics, Beijing Institute of Technology, Beijing, 100081, China (Email: jing.guo89@yahoo.com). S. Durrani and X. Zhou are with the Research School of Electrical, Energy and Materials Engineering, The Australian National University, Canberra, ACT 2601, Australia (Emails: {salman.durrani, xiangyun.zhou}@anu.edu.au).

This work was supported by the Australian Research Council's Discovery Project Funding Scheme (Project number DP170100939).

denote the path-loss exponent and fading power gain on the wireless link, respectively. We assume that the forward and backward links between the reader and a BN are reciprocal [5], [6], [10], [11] and all links experiences additive white Gaussian noise with variance σ^2.

Proposed collision reduction mechanism: We consider that time is divided into frames of duration $\mathcal{T}$ and each frame is further divided into T sub-frames. To efficiently reduce the collisions, we propose that each BN randomly and independently selects one sub-frame to access and communicate with the reader. In addition, each BN backscatters the signal if and only if the instantaneous received power is above a backscatter threshold ρ. The BNs satisfying the condition (i.e., $P_T h||x||^{-\alpha} \geq \rho$) are known as active BNs. A BN in backscatter phase varies its impedance to modulate and reflect the incident CW signal in order to access and communicate with the reader. The BNs not meeting the condition keep silent and are known as inactive BNs. Thus, each BN has two phases in one time frame, namely the backscatter phase (of duration $1/T$) and the waiting phase (of duration $(T-1)/T$). We refer to $1/T$ as the duty cycle. In this work, we focus on the backscatter phase.

We consider BPSK in this work and the reflection coefficient ξ is assumed to be the same for all BNs. Then the backscattered power at an active BN is $\xi P_T h||x||^{-\alpha}$ and the received power from an active BN at the reader is $P_T \xi h^2 ||x||^{-2\alpha}$.

SIC assumptions: For a certain sub-frame, there can be multiple active BNs accessing the reader simultaneously. To resolve the collisions, we employ SIC in this work. Similar to [7]–[9], we assume that the perfect channel state information for active BNs is available at the reader and adopt the stronger-to-weaker decoding order. Under this decoding order, the reader will first decode the strongest instantaneous received power and treat other signals as interference. If the SINR is greater than a SINR threshold γ, the strongest signal can be successfully decoded and extracted from the composite signal. The reader then proceeds to decode the second strongest signal and so on. We include the error propagation in this work. That is to say, if the j-th strongest signal fails to be decoded, the reader will stop decoding the succeeding signals. Furthermore, due to the constraint on computational complexity and delay, we assume that the total number of BNs whose signal can be decoded is limited to $N_{\max}$.

III. System Performance

A. Average Number of Decoded BNs in One Time Frame

The metric used to characterize the BackCom system performance is the average number of decoded BNs. It is defined as the average number of BNs whose information is successfully decoded by the reader in one time frame. Mathematically, it can be formulated as

$$\bar{K}_{\text{total}} = T\bar{K} = T\sum\nolimits_{j=1}^{N_{\max}} \mathsf{p}_{\text{suc},j}, \tag{1}$$

where $\bar{K}$ is the average number of BNs whose information is decoded successfully in one sub-frame and $\mathsf{p}_{\text{suc},j}$ is the average probability that j-th strongest signal is successfully decoded in one sub-frame.

In the following, we focus on the performance in one sub-frame. Note that selecting a sub-frame can be regarded as an independent thinning process for the original PPP Φ [12]. Hence, the location of BNs selecting one typical sub-frame is a PPP with density $\frac{1}{T}\bar{\lambda}||x||^b$ and we define $\tilde{\lambda} \triangleq \frac{1}{T}\bar{\lambda}$. The main challenge in (1) is determining $\mathsf{p}_{\text{suc},j}$. We first present the following four lemmas which help to evaluate $\mathsf{p}_{\text{suc},j}$. The proofs for these lemmas are presented in Appendix A.

Lemma 1: Let $\Xi = \{y_i\} \triangleq \{||x_i||^\alpha / h_i\}$ denote the path-loss and fading random process in one sub-frame. $P_T y_i^{-1}$ can be viewed as the received power at the i-th BN and we call y_i as the i-th node in Ξ. Then Ξ is a one-dimension PPP with density function $\lambda(y) = 2\pi\tilde{\lambda} y^{\tilde{b}-1}\mathbb{E}\left[h^{\tilde{b}}\right]/\alpha$ and intensity measure $\Lambda([0,y]) = 2\pi\tilde{\lambda} y^{\tilde{b}}\mathbb{E}\left[h^{\tilde{b}}\right]/(b+2)$, where $\tilde{b} \triangleq \frac{b+2}{\alpha}$ and $\mathbb{E}\left[h^{\tilde{b}}\right] = \Gamma\left[m+\tilde{b}\right] m^{-\tilde{b}}/\Gamma[m]$ when the channel experiences Nakagami-m fading. For the PPP Ξ, the number of nodes satisfying $y \leq \beta \triangleq P_T/\rho$, k, is a Poisson random variable with mean $\Lambda([0,\beta])$. Its probability mass function is

$$\Pr_K(k) = \left(\Lambda([0,\beta])\right)^k \exp\left(-\Lambda\left([0,\beta]\right)\right)/k!. \tag{2}$$

Lemma 2: For the PPP Ξ, the conditional probability density function (*pdf*) of the distance of the q-th nearest node to the origin, $y_{(q)}$, conditioned on $y_{(q)} \leq \beta \triangleq P_T/\rho$, is

$$f_{y_{(q)}|y_{(q)}\leq\beta}\left(y_{(q)}\right) = \frac{\tilde{b}\left(\Lambda([0,y_{(q)}])\right)^q}{(q-1)!y_{(q)}} \exp\left(-\Lambda([0,y_{(q)}])\right) \Big/ F_{y_{(q)}}(\beta), \tag{3}$$

where $0 \leq y_{(q)} \leq \beta$ and $F_{y_{(q)}}(\beta)$ is presented in (14). The bracket in the subscript indicates the nodes are ordered and $P_T\xi y_{(q)}^{-2}$ can be considered as the q-th strongest power received at the reader.

Lemma 3: Under the PPP $\Xi = \{y_i\}$, for any node satisfying $y_i \leq \beta$, the distribution of the distance between the node and the origin is i.i.d. and this conditional *pdf* is given by

$$f_{y|y\leq\beta}(y) = \tilde{b}y^{\tilde{b}-1}/\beta^{\tilde{b}}, \qquad 0 \leq y \leq \beta. \tag{4}$$

Lemma 4: Under the PPP $\Xi = \{y_i\}$, given that there are n_t nodes satisfying $y_i \leq \beta$, the conditional *pdf* of the distance from the q-th nearest node to the origin $y_{(q)}$ is

$$f_{y_{(q)}|n_t}\left(y_{(q)}\right) = \frac{n_t!\left(\frac{y^{\tilde{b}}}{\beta^{\tilde{b}}}\right)^{q-1}\left(1-\frac{y^{\tilde{b}}}{\beta^{\tilde{b}}}\right)^{n_t-q}\tilde{b}\frac{y^{\tilde{b}-1}}{\beta^{\tilde{b}}}}{(n_t-q)!(q-1)!}, \tag{5}$$

where $q \leq n_t$ and $0 \leq y_{(q)} \leq \beta$.

B. Performance Analysis

For the considered system setup, each decoding step under the SIC is correlated, e.g., whether the j-th strongest signal can be decoded successfully depends on whether the $j-1$-th strongest signal can be successfully decoded. For analytical tractability, we assume that each decoding step is independent [7]. The approximated result for $\mathsf{p}_{\text{suc},j}$ is presented in the following proposition.

Proposition 1: According to the system model in Section II, by assuming that each decoding step is independent, the

average probability that the j-th strongest signal is successfully decoded is approximated by

$$\mathsf{p}_{\text{suc},j} \approx \Pr_K(k \geq j) \prod_{t=1}^{j} \mathsf{p}_{\text{suc},t|k\geq j}(t,k,j), \tag{6}$$

where $\Pr_K(k \geq j)$ is the probability that the number of active BNs k in one sub-frame is equal or greater than j. Using *Lemma 1*, it is given by

$$\Pr_K(k \geq j) = 1 - \sum_{l=0}^{j-1} \Pr_K(l) = F_{y_{(j)}}(\beta). \tag{7}$$

In (6), $\mathsf{p}_{\text{suc},t|k\geq j}(t,k,j)$ is the conditional probability that the t-th strongest signal is successfully decoded, which is conditioned on that the number of active BNs k in one sub-frame is equal or greater than j. Note that the $t-1$ stronger signals are assumed to be successfully decoded and removed. It is expressed as

$$\mathsf{p}_{\text{suc},t|k\geq j}(t,k,j) = \frac{\Pr_K(k \geq t)\mathsf{p}^{\text{p}}_{\text{suc},t|k\geq t}(t) - \sum_{l=t}^{j-1} \Pr_K(l)\mathsf{p}^{\text{b}}_{\text{suc},t|k=l}(t,l)}{\Pr_K(k \geq j)}, \tag{8}$$

where $\mathsf{p}^{\text{p}}_{\text{suc},t|k\geq t}(t)$ is the conditional probability that the t-th strongest signal is successfully decoded, given that the number of active BNs k in one sub-frame is equal or greater than t, and $\mathsf{p}^{\text{b}}_{\text{suc},t|k=l}(t,l)$ is the conditional probability that the t-th strongest signal is successfully decoded, given that the number of active BNs k in one sub-frame is equal to l. The superscript p (or b) indicates that the derivation of the success probability is based on the PPP (or Binomial point process) model.

Remark 1: Our proposed framework used to calculate the intermediate result (i.e., $\mathsf{p}_{\text{suc},j}$) is totally different from the framework in [7] and it has not been considered in other literature as well.

By applying the derivation procedure in [7] to our system model, we have the average probability that the j-th strongest signal is successfully decoded approximated by

$$\mathsf{p}_{\text{suc},j} \approx \prod_{t=1}^{j} \mathsf{p}_{\text{suc},t}(t), \tag{9}$$

where $\mathsf{p}_{\text{suc},t}(t)$ is the probability that the t-th stronger signal is successfully decoded when ignoring whether the previous signals are successfully decoded or not. According to the derivation procedure in [7], we find that $\mathsf{p}_{\text{suc},t}(t) = \mathsf{p}^{\text{p}}_{\text{suc},t|k\geq t}(t)$. Note that the derivation in [7] neglects the case where the number of accessing BNs is less than t, which can cause the approximation to be less accurate. However, we have taken this case into account. The comparison between the results from our framework and the results based on [7] will be presented in Section IV.

$\mathsf{p}^{\text{p}}_{\text{suc},t|k\geq t}(t)$ and $\mathsf{p}^{\text{b}}_{\text{suc},t|k=l}(t,l)$ are two key factors determining $\mathsf{p}_{\text{suc},j}$. The success probability is generally defined as the average probability that the SINR at the typical BN is greater than the threshold. Since the decoding order for our SIC scheme is based on the instantaneous reflected power from the BN rather than the distance between the BN and the reader, we cannot compute the success probability leveraging the property of Nakagami-m fading on the typical link. Instead, we employ the moment generating function (MGF)-based approach to compute the two conditional success probabilities, which are presented in the following corollary.

Corollary 1: Based on the system model in Section II, these two success probabilities are given by

$$\mathsf{p}^{\text{p}}_{\text{suc},t|k\geq t}(t) = \Phi\left(\mathcal{M}_{(\mathsf{SINR}_{\text{p}}(t))^{-1}}(s)\right), \tag{10}$$

$$\mathsf{p}^{\text{b}}_{\text{suc},t|k=l}(t,l) = \Phi\left(\mathcal{M}_{\left(\mathsf{SINR}_{\text{b}(t,l)}\right)^{-1}}(s)\right), \tag{11}$$

where $\Phi(\mathcal{M}(s)) = 1 - \frac{\exp\left(\frac{A}{2}\right)}{2^B\gamma}\sum_{b=0}^{B}\binom{B}{b}\sum_{c=0}^{C+b}\frac{(-1)^c}{D_c}\text{Re}\left\{\frac{\mathcal{M}(s)}{s}\right\}$, $D_c = 2$ (if $c = 0$) and $D_c = 1$ (if $c = 1, 2, \ldots$), $s = (A + \mathbf{i}2\pi c)/(2\gamma)$ and $\text{Re}\{\cdot\}$ denotes the real part. The three parameters A, B and C are used to control the estimation error, which are set to $A = 10\ln 10$, $B = 15$, $C = 21$ [13]. $\mathcal{M}_{(\mathsf{SINR}_{\text{p}}(t))^{-1}}(s)$ and $\mathcal{M}_{\left(\mathsf{SINR}_{\text{b}(t,l)}\right)^{-1}}(s)$ are the MGF of the inverse SINR for the cases of the t-th strongest signal being decoded when the number of active BNs k is equal or greater than t or when $k = l$, respectively. Their expressions are given in (12) and (13) at the top of the next page, where $\Gamma[\cdot,\cdot]$ is the incomplete gamma function, $f_{y_{(t)}|y_{(t)}\leq\beta}\left(y_{(t)}\right)$ and $f_{y_{(t)}|l}\left(y_{(t)}\right)$ are given in *Lemma 2* and *Lemma 4*, respectively. *Proof:* See Appendix B.

In summary, combining (12) with (10) and (13) with (11) and then substituting $\mathsf{p}^{\text{p}}_{\text{suc},t|k\geq t}(t)$ and $\mathsf{p}^{\text{b}}_{\text{suc},t|k=l}(t,l)$ into (8), we obtain $\mathsf{p}_{\text{suc},t|k\geq j}(t,k,j)$. Then substituting (8) and (7) into (6), we obtain the approximated $\mathsf{p}_{\text{suc},j}$. Finally substituting $\mathsf{p}_{\text{suc},j}$ into (1), we work out the performance metric $\bar{K}_{\text{total}}$.

IV. Results

We present the results to study the considered BackCom system. Unless otherwise stated, consistent with existing literature, the parameters are set as: $b = -1$, $\bar{\lambda} = 0.5/\text{m}^2$, $\mathcal{T} = 50$, $\alpha = 3$, $m = 2$, $\sigma^2 = -100$ dBm, $P_T = 30$ dBm and $\xi = 0.6$.

Analysis validation: Fig. 1 plots the SINR threshold versus the average number of decoded BNs for $\rho = -10$ dBm and different $N_{\max}$. Note that $N_{\max}$ is defined in Section II and impacts the analysis as shown in (1). We set $T = \mathcal{T}/N_{\max}$ for the purpose of generating the results. The average number of accessing BNs in one time frame is the same, which is 63.96. This value is computed using $T \times \Lambda([0, P_T/\rho])$, where $\Lambda([0,\cdot])$ is given in *Lemma 1*. Fig. 1 shows that there is a small gap between the simulations and analytical results from our framework. We can see that the analysis is more accurate for lower SINR threshold, which is mainly governed by the independent decoding step assumption. In the low SINR region, the signals from the stronger users have very high chances to be successfully decoded (e.g., the success probability is close to 1) and consequently, whether the signals from weaker users are successfully decoded can be viewed as independent of the condition where the stronger users' signals are decoded successfully. This success probability is calculated exactly by us. Moreover, this independent approximation *in Proposition 1* is generally more accurate when $N_{\max}$ is smaller.

We also plot the analytical results based on [7] as discussed in *Remark 1*. Fig. 1 shows that, except for $N_{\max} = 1$, the

$$\mathcal{M}_{(\mathsf{SINR}_{\mathrm{p}}(t))^{-1}}(s)=\int_0^{\beta}\exp\left(-sy_{(t)}^2\frac{\sigma^2}{P_T\xi}\right)\exp\left(\frac{\pi\tilde{\lambda}\mathbb{E}\left[h^{\tilde{b}}\right]}{\alpha}\left(\left(\sqrt{s}y_{(t)}\right)^{\tilde{b}}\left(\Gamma\left[-\frac{\tilde{b}}{2},\frac{sy_{(t)}^2}{\beta^2}\right]-\Gamma\left[-\frac{\tilde{b}}{2},s\right]\right)-2\tilde{b}\left(\beta^{\tilde{b}}-y_{(t)}^{\tilde{b}}\right)\right)\right)$$
$$\times f_{y_{(t)}|y_{(t)}\leq\beta}\left(y_{(t)}\right)\,\mathrm{d}y_{(t)}. \tag{12}$$

$$\mathcal{M}_{\left(\mathsf{SINR}_{\mathrm{b}(t,l)}\right)^{-1}}(s)=\int_0^{\beta}\exp\left(-sy_{(t)}^2\frac{\sigma^2}{P_T\xi}\right)\left(\frac{\tilde{b}\left(\sqrt{s}y_{(t)}\right)^{\tilde{b}}}{2\left(\beta^{\tilde{b}}-y_{(t)}^{\tilde{b}}\right)}\left(\Gamma\left[-\frac{\tilde{b}}{2},\frac{sy_{(t)}^2}{\beta^2}\right]-\Gamma\left[-\frac{\tilde{b}}{2},s\right]\right)\right)^{l-t}f_{y_{(t)}|l}\left(y_{(t)}\right)\,\mathrm{d}y_{(t)}. \tag{13}$$

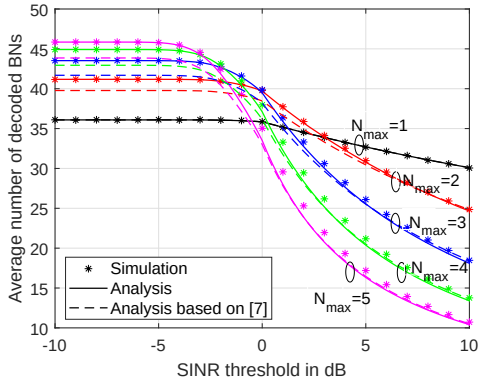

Fig. 1. Average number of decoded BNs $\bar{K}_{\text{total}}$ vs. SINR threshold γ.

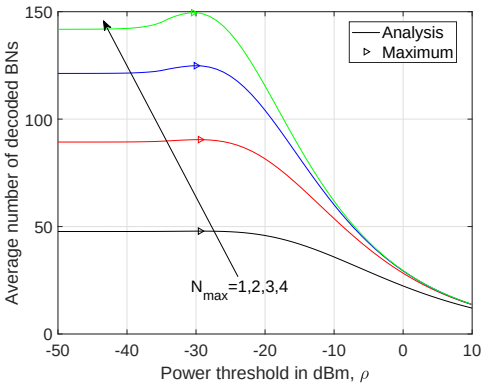

Fig. 2. Average number of decoded BNs $\bar{K}_{\text{total}}$ vs. backscatter threshold ρ.

results from [7] can deviate from the simulation results by a lot. This mainly comes from the fact that the derivation in [7] ignores that the number of accessing BNs can be less than the intended decoding BN number. This deviation is more obvious when the average number of accessing BNs is very small (e.g., the backscatter threshold is large). Hence, compared to the framework in [7], our framework can generally provide more accurate results in the relatively SINR threshold region and the scenario with smaller density of accessing BNs.

Effect of $N_{\max}$: From Fig. 1, under the assumption of $T=\mathcal{T}/N_{\max}$, we find that when the SINR threshold γ is small, a larger $N_{\max}$ results in better performance. When γ further increases, a smaller $N_{\max}$ can benefit the system. This is due to the interplay of the number of sub-frames T and the average number of decoded BNs in a sub-frame $\bar{K}$ from (1). When γ is small, the stronger signals are very likely to be decoded successfully and $\bar{K}$ plays the dominant role. A larger $N_{\max}$ indicates that there are more BNs accessing the reader, which leads to a large value of $\bar{K}$. Once γ becomes high, the signal is less likely to be decoded successfully and the impact of

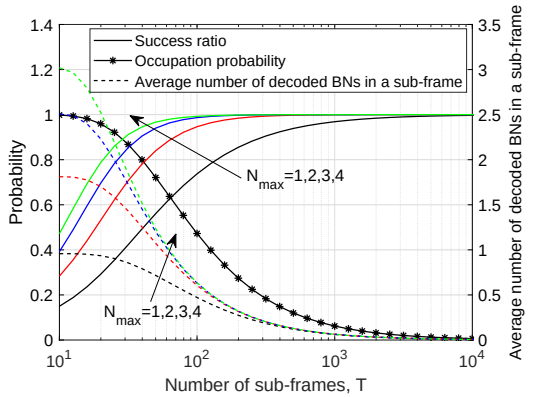

Fig. 3. The success ratio, occupation probability and average number of decoded BNs in a sub-frame $\bar{K}$ vs. number of sub-frames T.

error propagation is very severe, which leads to the similar performance of $\bar{K}$ for different $N_{\max}$.

Effect of number of sub-frames T: Fig. 3 plots (i) the number of sub-frames versus the success ratio defined as the ratio of average number of decoded BNs and the average number of accessing BNs (i.e., the solid curves), (ii) the occupation probability which is defined as the average probability that a sub-frame is occupied by BNs (i.e., the solid curve with star marks) and (iii) the average number of decoded BNs in a sub-frame $\bar{K}$ (i.e., the dashed curves) for different $N_{\max}$. According to Fig. 3, we can see that as T increases, the success ratio increases at first and then converges to 1. Meanwhile, $\bar{K}$ decreases and approaches zero. This can be explained as follows. With the increasing value of T, the average number of accessing BNs in a sub-frame decreases thereby reducing the interference. In other words, for a very large T value, since there are so many sub-frames, BNs are more likely to occupy different sub-frames and their signals have high chance to be decoded successfully due to little interference. Consequently, almost every accessing BN can be decoded successfully and the system achieves the best performance. Regarding the performance of $\bar{K}$, it is mainly governed by the occupation probability for large T. Clearly, this occupation probability (equivalently, $\bar{K}$) drops as T increases. From this figure, we find that, for the case of $N_{\max}=4$, in order to achieve 95% of the optimal performance, the sub-frame occupation probability is almost 80%; while the sub-frame occupation probability decreases to 18.31% in order to achieve 99.99% of the optimal performance. Consequently, this highlights the importance of carefully selecting the number of sub-frames such that it gives the near optimal performance while keeping the underutilization of sub-frames minimal.

Effect of backscatter threshold ρ: Fig. 2 plots the backscatter threshold versus the average number of decoded

$$\mathcal{M}_{\left(\mathsf{SINR}_{\mathrm{p}}(t)\right)^{-1}}(s)=\mathbb{E}_{y_{(t)},y_{(n)}}\left[\exp\left(-sy_{(t)}^{2}\left(\sum_{n=t+1}^{\infty}y_{(n)}^{-2}+\frac{\sigma^{2}}{P_{T}\xi}\right)\right)\right]=\mathbb{E}_{y_{(t)}}\left[\exp\left(-\frac{sy_{(t)}^{2}\sigma^{2}}{P_{T}\xi}-\int_{y_{(t)}}^{\beta}\left(1-\exp\left(-\frac{sy_{(t)}^{2}}{y^{2}}\right)\right)\lambda(y)\mathrm{d}y\right)\right]. \quad (15)$$

$$\mathcal{M}_{\left(\mathsf{SINR}_{\mathrm{b}(t,l)}\right)^{-1}}(s)=\mathbb{E}_{y_{(t)},y_{(n)}}\left[\exp\left(-sy_{(t)}^{2}\left(\sum_{n=t+1}^{l}y_{(n)}^{-2}+\frac{\sigma^{2}}{P_{T}\xi}\right)\right)\right]=\mathbb{E}_{y_{(t)}}\left[\exp\left(-\frac{sy_{(t)}^{2}\sigma^{2}}{P_{T}\xi}\right)-\left(\int_{y_{(t)}}^{\beta}\exp\left(-\frac{sy_{(t)}^{2}}{\hat{y}^{2}}\right)f_{\hat{y}}(\hat{y})\mathrm{d}\hat{y}\right)^{l-t}\right]. \quad (16)$$

BNs under $T=50$. We also mark the maximum $\bar{K}_{\text{total}}$ for each curve. From the figure, we find that, as ρ decreases, $\bar{K}_{\text{total}}$ first increases and then the curves become almost flat. When ρ is very large, a smaller number of BNs are allowed to access the reader and the performance of $\bar{K}_{\text{total}}$ is limited by the number of accessing BNs. As ρ increases, more BNs can access the reader, which initially enhances the system performance. However, it also brings in more collisions, which causes the drop of $\bar{K}_{\text{total}}$. When ρ further reduces, the increasing interference is negligible, which keeps curves almost unchanged.

V. Conclusion

In this work, we have investigated the average number of successfully decode BNs for a multiple access BackCom system with SIC technique. In order to reduce the access collision, we set a backscatter threshold for BNs in backscatter phase. Our results showed that this backscatter threshold has to be properly tuned to maximize the overall system performance. Overall, the considered system is effective in enabling multi-tag to reader communication.

Appendix A-Proof of Lemmas 1-4

Proof: (i) Lemma 1: The derivation follows the mapping displacement theorems of PPP [12, Sec 2.9.2.].

(ii) Lemma 2: According to Bayes' theorem, this conditional *pdf* is given by $\frac{f_{y_{(q)}}\left(y_{(q)}\right)}{F_{y_{(q)}}\left(y_{(q)}\right)}$, where $f_{y_{(q)}}\left(y_{(q)}\right)$ and $F_{y_{(q)}}\left(y_{(q)}\right)$ are the *pdf* and cumulative distribution function (*cdf*) of the distance from the q-th nearest node to the origin, respectively. The *cdf* of $y_{(q)}$ can be interpreted as the probability that there are at least q nodes closer than $y_{(q)}$ [14], i.e.,

$$F_{y_{(q)}}(y_{(q)})=1-\sum_{l=0}^{q-1}\frac{(\Lambda([0,y_{(q)}]))^{l}\exp\left(-\Lambda\left([0,y_{(q)}]\right)\right)}{l!}. \quad (14)$$

Then taking its derivative with respect to $y_{(q)}$ and after some manipulations, we arrive at (3).

(iii) Lemma 3: The condition *cdf* of y is $F_{y|y\leq\beta}(y)=\frac{\Lambda([0,y])}{\Lambda([0,\beta])}$. Then substituting the intensity function of $\Lambda([0,y])$ in *Lemma 1*, we have $F_{y|y\leq\beta}(y)=y^{\tilde{b}}/\beta^{\tilde{b}}$. Note that $f_{y|y\leq\beta}(y)=\frac{\mathrm{d}F_{y|y\leq\beta}(y)}{\mathrm{d}y}$. Hence, we obtain the conditional *pdf* of y in (4).

(iv) Lemma 4: For these n_t nodes satisfying $y_i\leq\beta$, their distance *pdf* $f_{y|y\leq\beta}(y)$ is i.i.d. and is presented in (4). Then following the statistical theory, we arrive at the conditional *pdf* for $y_{(q)}$ in (5). ■

Appendix B-Proof of Corollary 1

Proof: First consider $\mathcal{M}_{\left(\mathsf{SINR}_{\mathrm{p}}(t)\right)^{-1}}(s)$. The SINR's expression for this case can be written as $\mathsf{SINR}_{\mathrm{p}}(t)=P_{T}\xi y_{(t)}^{-2}/\left(\sum_{n=t+1}^{\infty}P_{T}\xi y_{(n)}^{-2}+\sigma^{2}\right)$. In fact, for these interfering nodes, their location follows the PPP with density $\lambda(y)=2\pi\tilde{\lambda}y^{\tilde{b}-1}\mathbb{E}[h^{\tilde{b}}]/\alpha$ outside the t-th node. Hence, we can express this MGF as in (15) at the top of this page, where the second step comes from the probability generating functional for a PPP [12]. Note that the distribution of $y_{(t)}$ here is $f_{y_{(t)}|y_{(t)}\leq\beta}\left(y_{(t)}\right)$ given in *Lemma 2*. After substituting $\lambda(y)$ and further calculation, we obtain the result in (12).

For $\mathcal{M}_{\left(\mathsf{SINR}_{\mathrm{b}(t,l)}\right)^{-1}}(s)$, the SINR for this case is $\mathsf{SINR}_{\mathrm{b}}(t,l)=P_{T}\xi y_{(t)}^{-2}/\left(\sum_{n=t+1}^{l}P_{T}\xi y_{(n)}^{-2}+\sigma^{2}\right)$. According to [15] and *Lemma 3*, the $l-t$ interfering nodes are i.i.d. with distribution $f_{\hat{y}}(\hat{y})=\tilde{b}\frac{\hat{y}^{\tilde{b}-1}}{\beta^{\tilde{b}}-y_{(t)}^{\tilde{b}}}$ and $y_{(t)}\leq\hat{y}\leq\beta$. Hence, we can express this MGF as shown in (16) at the top of this page, where the distribution of $y_{(t)}$ here is $f_{y_{(t)}|l}\left(y_{(t)}\right)$ given in *Lemma 4*. With further computation, we arrive at (13). ■

References

[1] W. Liu, K. Huang, X. Zhou, and S. Durrani, "Next generation backscatter communication: Theory and applications," *EURASIP Journal on Wireless Communications and Networking*, pp. 1–11, Mar. 2019.

[2] Y. Zhang, F. Gao, L. Fan, X. Lei, and G. K. Karagiannidis, "Backscatter communications over correlated nakagami-m fading channels," *IEEE Trans. Commun.*, vol. 67, no. 2, pp. 1693–1704, Feb. 2019.

[3] A. Bletsas, S. Siachalou, and J. N. Sahalos, "Anti-collision backscatter sensor networks," *IEEE Trans. Wireless Commun.*, vol. 8, no. 10, pp. 5018–5029, Oct. 2009.

[4] J. Wang, H. Hassanieh, D. Katabi, and P. Indyk, "Efficient and reliable low-power backscatter networks," in *Proc. ACM SIGCOMM*, 2012, pp. 61–72.

[5] G. Yang, C. K. Ho, and Y. L. Guan, "Multi-antenna wireless energy transfer for backscatter communication systems," *IEEE J. Sel. Areas Commun.*, vol. 33, no. 12, pp. 2974–2987, Dec. 2015.

[6] J. Guo, X. Zhou, S. Durrani, and H. Yanikomeroglu, "Design of non-orthogonal multiple access enhanced backscatter communication," *IEEE Trans. Wireless Commun.*, vol. 17, no. 10, pp. 6837–6852, Oct. 2018.

[7] C. Psomas and I. Krikidis, "Backscatter communications for wireless powered sensor networks with collision resolution," *IEEE Wireless Commun. Lett.*, vol. 6, no. 5, pp. 650–653, Oct. 2017.

[8] X. Zhang and M. Haenggi, "The performance of successive interference cancellation in random wireless networks," *IEEE Trans. Inform. Theory*, vol. 60, no. 10, pp. 6368–6388, Oct. 2014.

[9] M. Wildemeersch, T. Q. S. Quek, M. Kountouris, A. Rabbachin, and C. H. Slump, "Successive interference cancellation in heterogeneous networks," *IEEE Trans. Commun.*, vol. 62, no. 12, pp. 4440–4453, Dec. 2014.

[10] W. Liu, K. Huang, X. Zhou, and S. Durrani, "Full-duplex backscatter interference networks based on time-hopping spread spectrum," *IEEE Trans. Wireless Commun.*, vol. 16, no. 7, pp. 4361–4377, Jul. 2017.

[11] D. Mishra and E. G. Larsson, "Optimal channel estimation for reciprocity-based backscattering with a full-duplex MIMO reader," *IEEE Trans. Signal Process.*, vol. 67, no. 6, pp. 1662–1677, Mar. 2019.

[12] M. Haenggi, *Stochastic Geometry for Wireless Networks*. Cambridge University Press, 2012.

[13] J. Guo, S. Durrani, and X. Zhou, "Outage probability in arbitrarily-shaped finite wireless networks," *IEEE Trans. Commun.*, vol. 62, no. 2, pp. 699–712, Feb. 2014.

[14] M. Haenggi, "On distances in uniformly random networks," *IEEE Trans. Inform. Theory*, vol. 51, no. 10, pp. 3584–3586, Oct. 2005.

[15] M. Afshang, H. S. Dhillon, and P. H. J. Chong, "Modeling and performance analysis of clustered device-to-device networks," *IEEE Trans. Wireless Commun.*, vol. 15, no. 7, pp. 4957–4972, July 2016.